Supplementary Materials for

Filament Rigidity and Connectivity Tune the Deformation Modes of Active Biopolymer Networks

Samantha Stam[1,2], Simon L. Freedman[3,6], Shiladitya Banerjee[3,4,5], Kimberly L. Weirich[3], Aaron R. Dinner[2,3,7] and Margaret L. Gardel[2,3,6]

MATERIALS & METHODS

Protein purification

Actin was purified from rabbit acetone powder (Pel-Freez Biologicals, Rogers, AR) with a protocol derived from (48) and stored as a monomer in G-buffer (2 mM Tris HCl pH 8.0, 0.2 mM ATP, 0.2 mM $CaCl_2$, 0.2 mM DTT, 0.005% NaN_3). Fluorescent labeling of actin was done with a tetramethylrhodamine-6-maleimide dye (Life Technologies, Carlsbad, CA). Skeletal muscle myosin II was purified from chicken breast (49) and labeled with Alexa-642 maleimide (Life Technologies, Carlsbad, CA) (50). Filamin was purified from chicken gizzard (51). Fascin was purified using a GST-tagged construct (52) and Dave Kovar lab, University of Chicago). Purification was done using a glutathione sepharose column (GE Healthcare Life Sciences). The GST tag was then cleaved with thrombin (GST Healthcare Life Sciences) and separated by chromatography (Hi-Trap Q column; GE Healthcare Life Sciences).

Microscopy sample preparation

The coverslip surface was passivated against non-specific adhesion of protein with a surfactant layer, either a lipid bilayer (53) or a fluorinated oil-surfactant layer (17). To prepare a lipid bilayer, coverslips (#1.5, Fisherbrand) were rinsed with water and ethanol, then exposed to UV-ozone for 20 minutes. The sample chamber was assembled by anchoring a glass cylinder (cat# 3166-10; Corning Life Sciences, Corning, NY) to the coverslip with vacuum grease. This was filled with vesicle buffer (10 mM phosphate buffer, pH 7.5, 140 mM sodium chloride) and DOPC vesicles (1,2-dioleoyl-*sn*-glycero-3-phosphocholine, Avanti Polar Lipids, Alabaster, AL) were added to a concentration of 100 µM and incubated for 15 minutes to allow bilayer formation. To prepare the oil-surfactant surface, PFPE-PEG-PFPE surfactant (cat # 008, RAN Biotechnologies, Beverly, MA) was dissolved to a concentration of 2% w/w in Novec-7500 Engineered Fluid (3M, St Paul, MN). Coverslips were cleaned by sonication in water and ethanol, immersed in a 2% v/v solution of triethoxy(octyl)silane (cat# 440213; Sigma-Aldrich, St. Louis, MO) in isopropanol, and rinsed thoroughly to produce a hydrophobic surface. To constrain the oil to a small region and prevent seeping and flow from the chamber edges, a 2x2 mm Teflon mask was placed on the coverslip before exposing the coverslip to UV/ozone for 10 minutes. This removed the hydrophobic silane treatment from all surrounding areas of the coverslip. The sample chamber was then constructed, similarly as with the bilayer surface, by adhering a glass cylinder to the coverslip using epoxy. The surface of the coverslip within the cylinder was coated with the oil-surfactant solution, and the actin polymerization mixture was immediately added.

The actin polymerization mixture consisted of an oxygen scavenging system to prevent photobleaching (4.5 mg/mL glucose, 2.7 mg/mL glucose oxidase (cat#345486, Calbiochem, Billerica, MA), 1700 units/mL catalase (cat#02071, Sigma, St. Louis, MO), and 0.5 v/v % β-mercaptoethanol), and 0.3% w/w 15 cP methylcellulose (15) in 1x F-

buffer (10 mM imidazole, pH 7.5, 1 mM MgCl2, 50 mM KCl, 0.2 mM EGTA, 4 mM ATP). Actin from frozen stocks in G-buffer (above) was added to a final concentration of 1 μM with a ratio of 1:10 TMR-maleimide labeled:unlabeled actin monomer. Polymerization of actin was allowed to proceed for 30 minutes. For bundled samples, fascin stored in 20 mM Tris-HCl, pH 8, 10% glycerol, 100 mM NaCl, 0.2 mM EDTA, 0.01% NaN3 was then added at a ratio of 1:10 fascin:actin monomer and allowed to form bundles for 20 minutes. Similarly, filamin (10 mM Tris-HCl, pH 7.4, 1 mM EDTA, 1 mM DTT, 2 mM MgCl2, 120 mM NaCl) was added at a ratio of 1:500 filamin: actin monomer and allowed to crosslink for 20 minutes. Monomeric myosin II was polymerized into myosin filaments separately in the same buffer conditions for 10 minutes and added at a ratio of 1:13 myosin monomer:actin monomer.

Fluorescence microscopy

Images were obtained using an inverted microscope (Eclipse Ti-E; Nikon, Melville, NY) with a spinning disk confocal head (CSU-X; Yokagawa Electric, Musashino, Tokyo, Japan) and CMOS camera (Zyla-4.2-USB3; Andor, Belfast, UK). A 40x 1.15 NA water-immersion objective (Apo LWD; Nikon) was used for all imaging. Images were collected every 1 s using 568 nm and 647 nm excitation for the actin and myosin respectively. Image acquisition was under automated control by Metamorph (Molecular Devices, Sunnyvale, CA).

Image Analysis

Images were aligned using the StackReg (http://bigwww.epfl.ch/thevenaz/stackreg/) (54) plugin of ImageJ (https://imagej.nih.gov/ij/) (55) to remove drift. Background intensity was subtracted using the built-in Subtract Background plugin of ImageJ. The myosin particle density was calculated in ImageJ and actin velocity vectors were calculated using particle imaging velocimetry software (http://www.oceanwave.jp/softwares/mpiv/). The grid size used for PIV vector calculation was 2.4 μm except for the systematic variation in Supplemental Fig. S6. All further analysis was done using custom Matlab scripts.

All experimental image analysis plots that report values at different times were smoothed such that each data point represents the average over overlapping 20 s time windows. The values of the contractile moment at different length scales in Fig. 1J, and Fig. 6D were averaged for 30 s starting with the time points of maximal magnitude of $<\nabla \cdot \vec{v}_{act}>$ given by the asterisks in Fig. 1I and Fig. 6C. The rescaling of quantities in Fig. 3 and Fig S4 was done such that their range spans from 0 to 1, e.g., $l_{corr} = \frac{L_{corr} - min(L_{corr})}{\max(L_{corr})}$.

Simulation methods

We used AFiNeS, a software package that we developed for simulating active polymer networks (28), to systematically vary actin flexibility and cross-linker density in two-dimensional networks of F-actin, myosin, and cross-linkers. These components were

initially placed at random locations in a 50 μm $\times$ 50 μm box with periodic boundary conditions and evolved via overdamped Langevin dynamics for 200 s. We ran four replicates of 77 simulations, each with different crosslink density (ρ_{xl}) varying between 0 and 1 μm^{-2} and filament rigidity (κ_B) varying between 0 and 1 pNμm^2. A complete list of parameter values is available in Table 1 of the Supplemental Information. The divergence calculation in Fig. 4C is weighted by the local actin density because the experimental PIV method does not calculate vectors at locations below a threshold actin density.
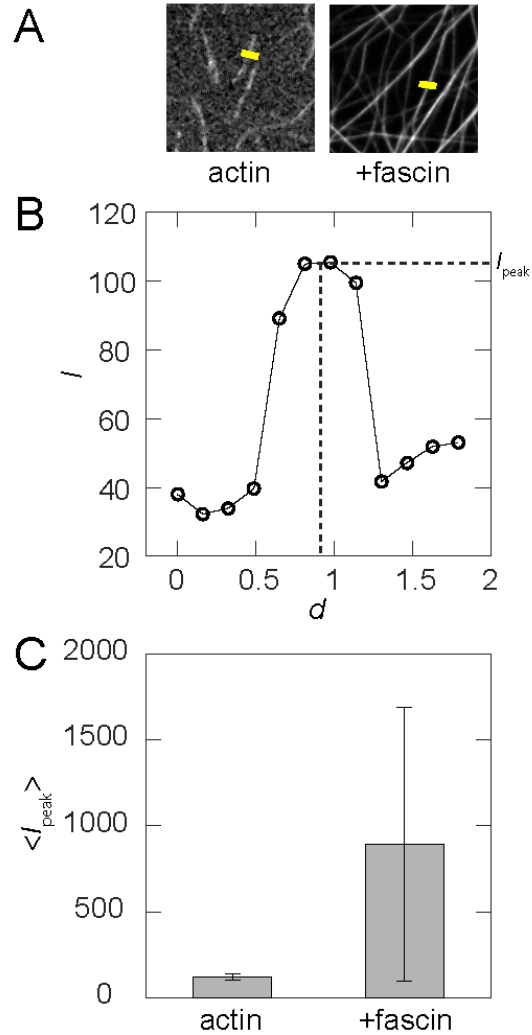
Supplemental Figure S1: Fascin bundles contain ~ 8 actin filaments

(A): Intensity scans are taken along lines perpendicular to indiviudual actin filaments (left) and rigid fasin bundles (right). (B) The resulting intensity profile has a peak intensity, I_{peak}. (C) The average value of I_{peak} for fascin bundles is approximately 8 times that of individual filaments.
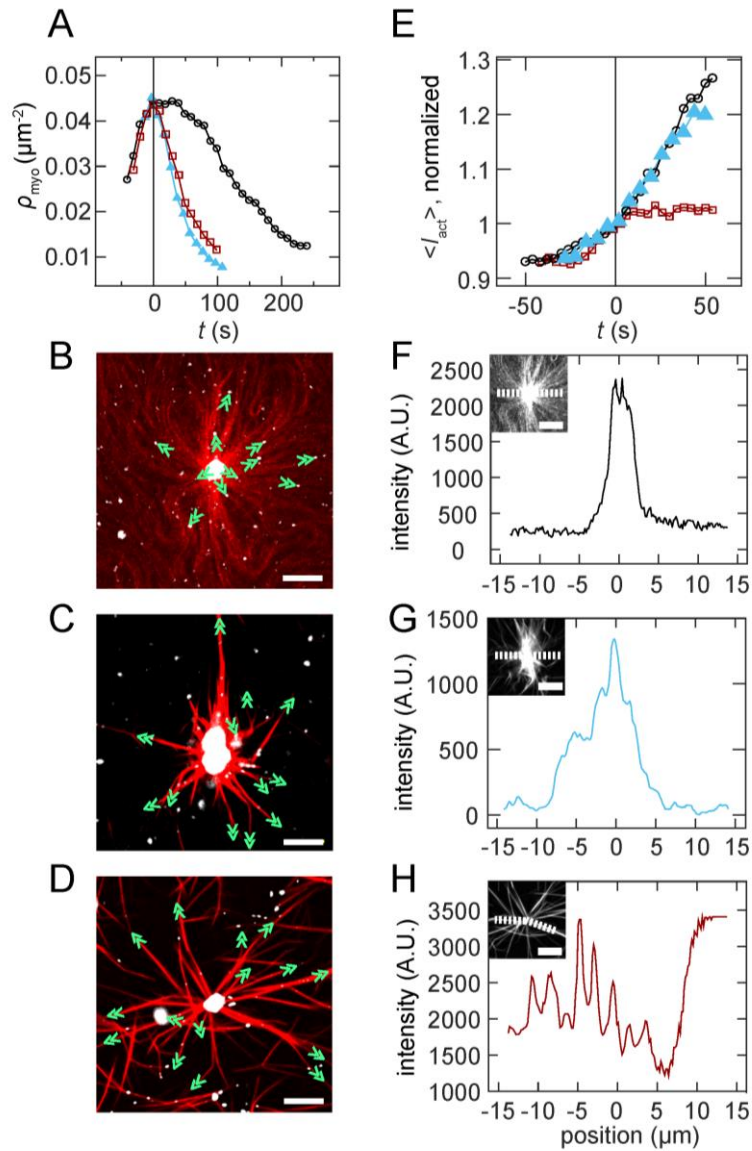
Supplemental Figure S2: Networks form polarity-sorted asters with varying structure

(A): Time $t = 0$ defines the peak myosin cluster density after myosin filaments accumulate on the surface and begin to coalesce in semi-flexible filament network (open black circles), cross-linked rigid bundles (1:10 fascin:actin, 1:500 filamin:actin, filled blue triangles), and rigid bundles without cross-links (1:10 fascin:actin open red squares). (B-D): By tracking the motion of myosin on bundles/filaments that emanate from the aster, the local polarity is assessed and marked on images with the open end of the chevron indicating the direction of motion and direction of barbed end. Aster polarity in (B) semi-flexible filament network, (C) cross-linked rigid bundles (1:10 fascin:actin, 1:500 filamin:actin) and (D) rigid bundles without cross-links (1:10 fascin:actin). (E): $<I_{act}>$ in each frame is calculated by averaging the actin over all pixels that exceed a background threshold, and then normalizing by the value at time t = 0. Densification of actin, indicated by a rise in this value, occurs in semi-flexible filament (open black circles) and cross-linked rigid bundle (filled blue triangles) while rigid bundles without cross-links are rearranged without densification (open red squares). (F)-(H): Intensity scans of clusters formed in the compressible filament (D), cross-linked rigid bundle (E) and uncross-linked rigid bundle (F) networks. As a consequence of the densification illustrated in (E), actin is highly concentrated in the center of the asters in (F) and (G). In contrast, the aster in (H) has intensity peaks diffusively spread throughout the structure. Scale bars on insets are 10 µm.
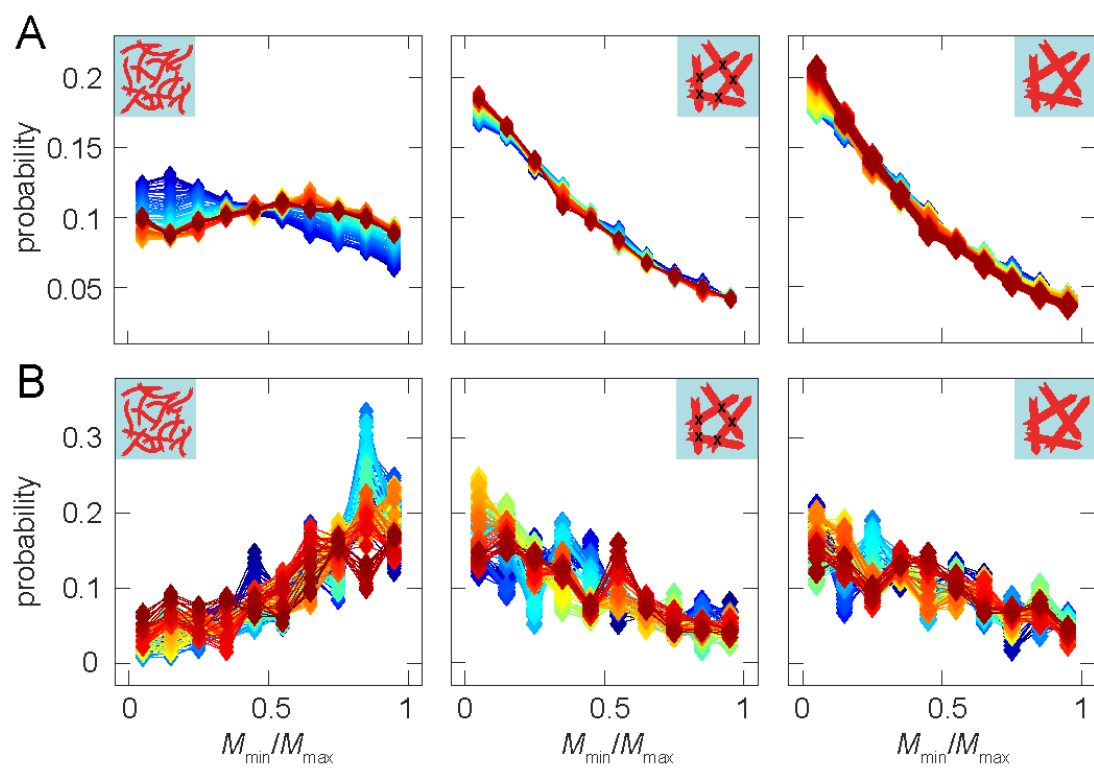
Supplemental Figure S3: Networks have different contributions of biaxial and uniaxial deformations at varying length scales

(A): Distributions of M_{min}/M_{max} with $s = 6$ μm for network of semi-flexible filaments, cross-linked rigid bundles, and uncross-linked rigid bundles from left to right. (B): Distributions of M_{min}/M_{max} for same samples as (A) with $s = 60$ μm.
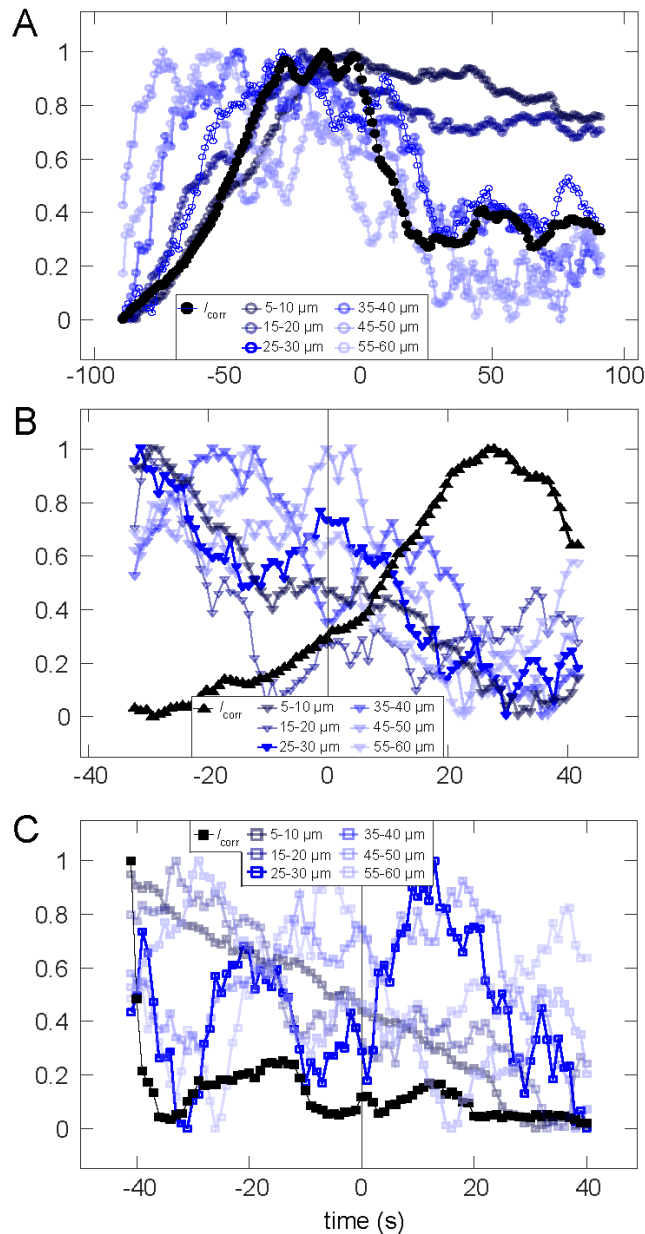
Supplemental Figure S4: $P_{biaxial}$ **at varying length scales has different trends over time for different networks.**

(A): $P_{biaxial}$ values at all varying length scales, s, (open blue circles, legend indicates value of s) initially increases and then decreases in network of semi-flexible filaments. At an intermediate value of s, the trend follows that of the correlation length, L_{corr} (filled black circles). (B): $P_{biaxial}$ at varying s (open blue triangles) decreases upon addition of myosin in network of cross-linked rigid bundles, while L_{corr} (filled black circles) increases. (C): $P_{biaxial}$ (open blue squares) at small s decreases after myosin addition in network of uncross-linked bundles but does not have a clear trend on longer length scales. Unlike the other two networks, L_{corr} decreases after myosin addition (filled black squares). For all curves, the values are shifted and scaled to range from 0 to 1.

7
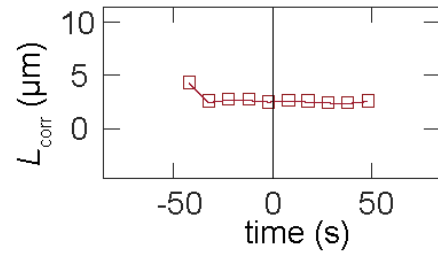
Supplemental Figure S5: Data for network of rigid bundles without cross-links.

Unscaled L_{corr} as a function of time.
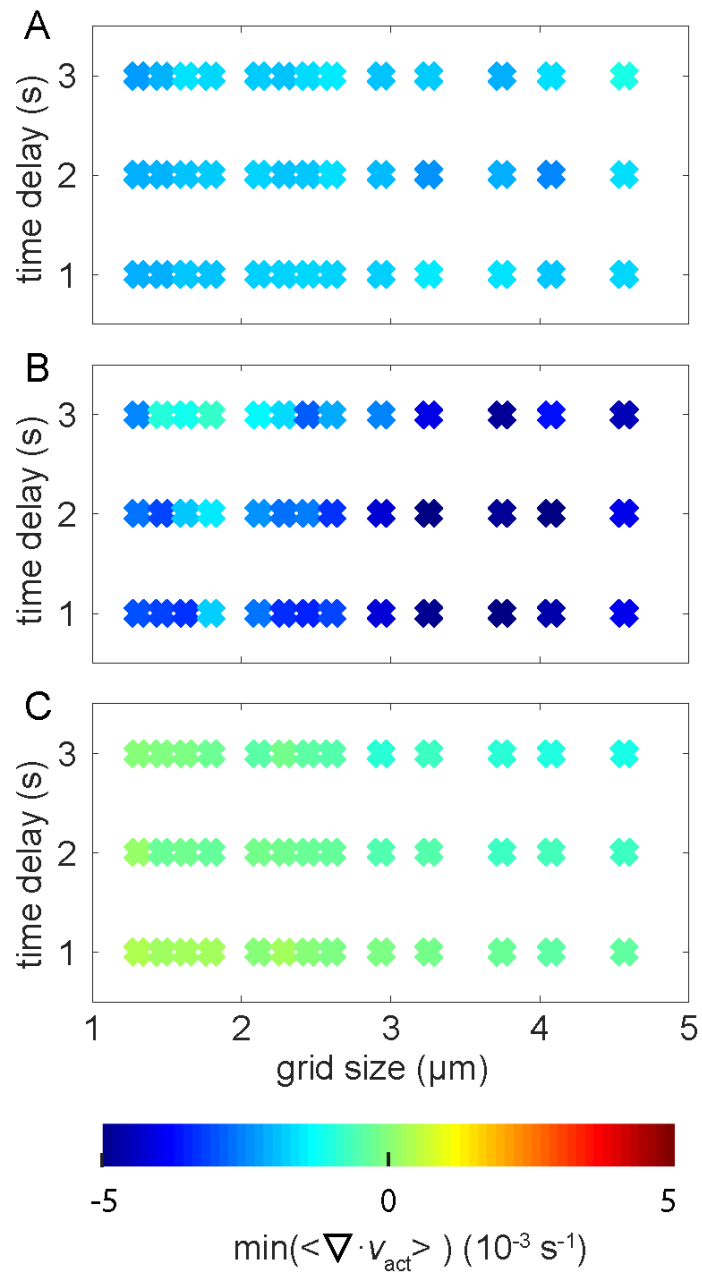
Supplemental Figure S6: Minimum of $<\nabla \cdot \vec{v}_{act}>$ for PIV vectors calculated with varying time delay and length scale

The minimum of the spatially averaged divergence is indicated by the color scale for semi-flexible filaments (A), cross-linked rigid bundles (B), and rigid bundles without cross-links (C).

Symbol	Description (unit)	Value
	Actin filaments	
N_F	Number of filaments	500
N_B	Number of links per filament	10
l_a	Link rest length (μm)	1
k_a	Filament link stiffness ($pN/\mu m$)	1
κ_B	Bending modulus ($pN\mu m^2$)	[0.001,1]
	Myosin motors	
ρ_m	Density (μm^{-2})	[0, 1]
l_m	Rest length (μm)	1
k_m	Stiffness ($pN/\mu m$)	1
k_m^{on}	Max attachment rate (s^{-1})	1
k_m^{off}	Max detachment rate (s^{-1})	0.1
v_0	Unloaded speed ($\mu m/s$)	1
F_s	Stall force (pN)	10
	Filamin crosslinkers	
ρ_{xl}	Density (μm^{-2})	1
k_{xl}	Stiffness ($pN/\mu m$)	1
k_{xl}^{on}	Max attachment rate (s^{-1})	1
k_{xl}^{off}	Max detachment rate (s^{-1})	0.1
	Environment	
Δt	Dynamics timestep (s)	0.00002
t_f	Total simulated time (s)	200
X, Y	Length and width of assay (μm)	50
g	Grid density (μm^{-2})	1
T	Temperature (K)	300
ν	Dynamic viscosity ($Pa * s$)	0.001

Supplemental Table S1: Full list of simulation parameters

Supplementary Movie Captions

Movie S1
Timelapse images of TMR-actin (red) and Alexa-642 myosin (white) in sample with no actin cross-linker. Time stamp is in minutes:seconds format and 0:00 indicates the time of the maximal density of myosin puncta.

Movie S2
Timelapse images of TMR-actin (red) and Alexa-642 myosin (white) in sample containing fascin (1:10 fascin:actin monomer) and filamin (1:500 filamin:actin monomer). Time stamp is in minutes:seconds format and 0:00 indicates the time of the maximal density of myosin puncta.

Movie S3
Timelapse images of TMR-actin (left) and corresponding distribution of M_{min}/M_{max} (right, colors indicating time) in network with no cross-linker. Each M_{min}/M_{max} distribution curve is cumulative over a 20-frame window (time between frames = 1 s), and the actin image displayed for each curve occurs in the middle (10th frame) of this window.

Movie S4
Timelapse images of TMR-actin (left) and corresponding distribution of M_{min}/M_{max} (right, colors indicating time) in sample containing fascin (1:10 fascin:actin monomer) and filamin (1:500 filamin:actin monomer). Each M_{min}/M_{max} distribution curve is cumulative over a 20-frame window (time between frames = 1 s), and the actin image displayed for each curve occurs in the middle (10th frame) of this window.

Movie S5
Simulation images of semi-flexible filaments (red) and myosin (white) where $L_p = 25\ \mu$m and $\rho_{xl} = 1\ \mu$m^{-2}. Time delay between frames is 1 s.

Movie S6
Simulation images of rigid filaments (red) and myosin (white) where $L_p = 250\ \mu$m and $\rho_{xl} = 1\ \mu$m^{-2}. Time delay between frames is 1 s.

Movie S7
Timelapse images of TMR-actin (red) and Alexa-642 myosin (white) in sample containing fascin (1:10 fascin:actin monomer) and no filamin. Time stamp is in minutes:seconds format and 0:00 indicates the time of the maximal density of myosin puncta.

Movie S8
Timelapse images of TMR-actin (left) and corresponding distribution of M_{min}/M_{max} (right, colors indicating time) in sample containing fascin (1:10 fascin:actin monomer) and no filamin. Each M_{min}/M_{max} distribution curve is cumulative over a 20-frame window (time between frames = 1 s), and the actin image displayed for each curve occurs in the middle (10th frame) of this window.